Investigation for fuel-cell structures with multi-scale X-ray analysis

Kazuhiko Omote*, Tomoyuki Iwata*, Yoshihiro Takeda** and Joseph D. Ferrara***

1. Introduction

It is well known that X-rays have wavelengths comparable with interatomic distances and can be utilized for atomic-scale structural determination. In addition, X-rays can penetrate through opaque objects and show the internal structure without destroying the object. It is for these reasons that X-rays are widely used for atomic-scale structural analysis of various kinds of crystals including small molecules and large protein molecules[1], and in some cases providing accurate electron density information[2]. In addition, small-angle and ultra small-angle X-ray scattering (SAXS, USAXS) is an exceptionally useful technique for evaluating the size, shape, and morphology of higher-order structures in the range of a few nanometers to sub-micrometers[3]. Recently, the resolution of X-ray microscopes has been pushed down to the sub-micrometer level. These devices are also capable of recording computed tomography (CT) data[4],[5]. This is a powerful technique for visualizing the internal structure of various specimens in three dimensions (3D) at the micrometer scale. By utilizing these X-ray techniques, we have the opportunity to investigate a very extended range of multi-scale structures from the atomic-scale (10^{-10} m) to macroscopic-scale (10^{-2} m), continuously for various kinds of materials without destroying the specimens.

In this paper, we will investigate multi-scale structures of a polymer electrolyte membrane (PEM) fuel cell, which generates electricity with catalyst nanoparticles and its support, a proton exchange membrane, a micro-porous layer, a gas diffusion layer, and channels on separator. The sizes of those constituents are spread over nanometers to millimeters and providing the possibility to investigate using state-of-the-art X-ray analysis techniques. Figure 1 shows a sectional view of the PEM fuel cell[6]. The incoming hydrogen gas (H_2) passes through the gas diffusion layer (GDL), reacts on the catalyst (nanometer scale metal particles) and is oxidized at the anode catalyst layer. The electrons flow to an external load through the anode (negative) electrode and protons (H^+) are transferred to the cathode catalyst layer through PEM. The transferred protons are reacted on the cathode catalyst with oxygen and electrons, and generate water (H_2O). The oxygen gas passes through the cathode GDL and electrons come from the cathode (positive) electrode. Overall, oxygen and hydrogen gases are input and electric current and water are generated. The generated electric current from the fuel cell may be used to power devices. Fuel cells have the potential to reduce human energy use and a great deal of effort has been made to improve the performance (efficiency, lifetime, reliability, stability, etc.). For example, in order to accelerate the cathode and anode reactions, it is important to supply oxygen and hydrogen gases to the catalysts and the generated electrons should be collected by the anode electrode and supplied to the cathode electrode. Therefore, it is important the pores for supply enough gas-flow while maintaining electron current paths through the support of the catalyst. Thus, porous graphite materials having pore sizes on the order of several tens of nanometers are utilized. The other key material is the proton exchange membrane, which provides both proton transport from anode to cathode and acts as a barrier to the inter-diffusion of reacting gases (oxygen and hydrogen). Efficient proton transport is directly related to electric power generation and a number of studies have been carried to improve proton conductivity[7]. Gas diffusion layers sandwiching catalyst layers on both sides are made from carbon fibers a few micrometers in diameter. Those micrometer structures are expected to maintain an effective supply of reacting gases and discharge of the water product. The above combination is called the membrane electrode assembly (MEA). One MEA can generate a potential of one volt or less and, in practice, a stack of several hundred of MEAs is required. Therefore, the MEA is sandwiched by separators that have millimeter size channels to allow for the flow of

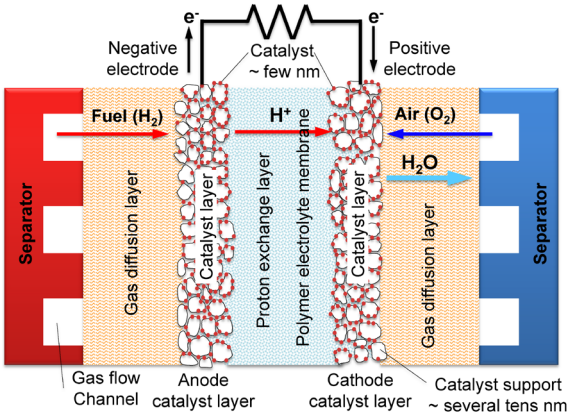

Fig. 1. Schematic view of fuel cell structure.

* X-ray Research Laboratory, Rigaku Corporation.
** SBU-PDX/TFX, X-ray Instrument Division, Rigaku Corporation.
*** Rigaku Americas Corporation.

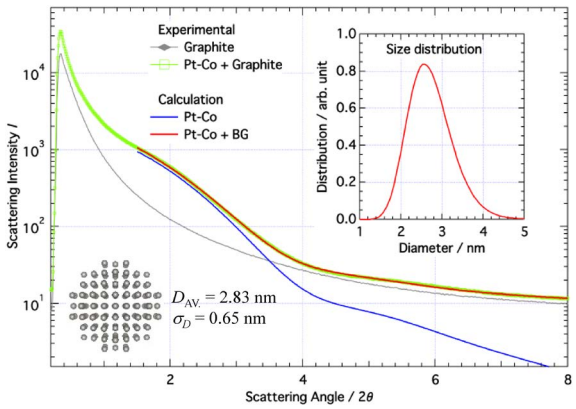

Fig. 2. Small angle scattering from catalyst particle on graphite support. Green line is the experimental and red line is the calculated profile. Inset is size distribution of the particle fitted to the experimental profile.

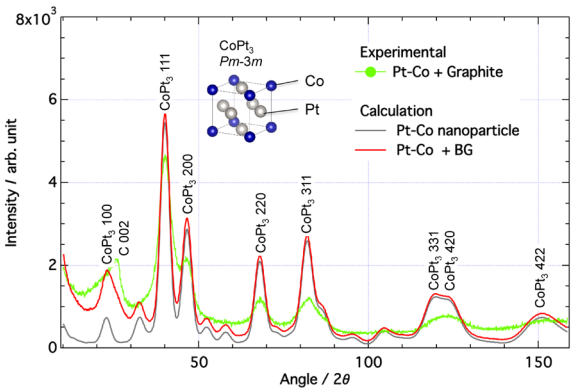

Fig. 3. Experimental and calculated X-ray diffraction patterns for Pt–Co nanoparticle with the size of 2.82 nm in diameter which is determined by small angle scattering shown in Fig. 2.

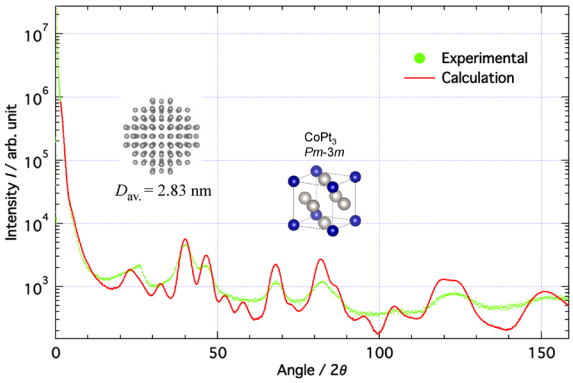

Fig. 4. Comparison of experimental and calculated profiles of small to wide-angle scattering/diffraction, assuming ideal atomic arrangement in the nanoparticle. The wider peak width of the experimental pattern means deformation of crystal structure of the nanoparticles.

gases and water as shown in Fig. 1.

In brief, a fuel cell operates based on reactions on nanometer-size catalysts and requiring transport of hydrogen gas, oxygen gas, protons, and electrons. Proton transport is restricted by the nanometer-scale membrane structure, electron current depends on conductivity of support of catalyst, and gas flows are affected by micrometer scale gas diffusion layers. In this paper, we will describe some results of our X-ray analysis with several different techniques for studying different levels of fuel cell structures. We will explain the results from small to large scales in the following sections.

2. Nanometer scale structural analysis with X-ray diffraction/scattering

2.1. Structure of catalyst nanoparticle

The polymer electrolyte membrane fuel cell has several superior features that allow it to operate at temperatures lower than 100°C, provide for a rapid warm up time, and generate electricity over a wide range of current density. It is for these reasons that the PEM fuel cell is already commercially available for residential use as a source of electricity and has been extensively studied for automotive applications. For the popular commercial use, it is important to reduce cost of the fuel cell. The most expensive material in the fuel cell is the catalyst, which is made from expensive Pt metal or a Pt alloy. The use of nanoparticles of a few nanometers in diameter decreases the total mass of Pt while maintaining the same active surface area. It is necessary to react three components, protons (H^+) penetrating through the PEM, oxygen molecules (O_2), and electrons (e^-) from the anode on the cathode catalyst. The reaction speed should be a rate-limiting process for generating electricity from the fuel cell. Furthermore, oxygen atoms can be the cause of degradation of the catalyst and its support materials, *e.g.* formation of metal oxide (MO_x) and evaporation of the graphite support (CO_x). In order to overcome those problems, Toda *et al.* made an extensive study and proposed candidates of several Pt alloy materials containing Fe, Ni, and Co instead of pure Pt. They have proven that certain compositions of those metals with Pt can greatly improve the reactivity of the catalyst[8]. A number of *in operando* studies of catalyst structures during fuel cell operation have been carried out using X-ray absorption fine structure at synchrotron facilities and elution of catalyst particles have been investigated[9].

In this section, we will explain our small angle X-ray scattering (SAXS) and wide angle scattering (WAXS) results for the Pt–Co alloy catalyst on a graphite support. Figure 2 shows experimental and calculated SAXS profiles of the specimen. The gray line indicates the measured SAXS profile from graphite support and the green line shows the SAXS profile for Pt–Co catalyst on the support. The contribution of the nanoparticles is clearly observable from 1° to 4° in 2θ. We have calculated the SAXS profile from Pt–Co nanoparticle that is indicated by blue line and adding a graphite contribution to fit the observed profile. The result is shown by the red curve, which agrees well with the experimental profile indicated by the green line.

The observed particle size distribution curve is also shown in the inset of Fig. 2. The mean diameter of the nanoparticles is 2.83 nm with a sigma of 0.65 nm.

We have further investigated crystal structure of the nanoparticle with powder X-ray diffraction measurement for the same sample (nanoparticle on graphite support). The results are shown as a green curve in Fig. 3. We could identify the crystal structure of the nanoparticles as $CoPt_3$ in space group $Pm\bar{3}m$, in which Pt and Co atoms are located at the ordered positions. The gray line in this figure is the calculated pattern assuming this crystal structure of $CoPt_3$ and particle size of 2.83 nm in diameter. The latter was estimated by the SAXS analysis. The red line is the calculated crystal diffraction pattern plus observed graphite support (without catalyst nanoparticle) scattering. Here we can see the observed peak positions agree well with that of calculated peak positions. On the other hand, the observed peak widths are wider than that of calculated peak widths, even assuming the observed particle size distribution. The peak width increases for the higher-order diffraction peaks. This means the crystal structure of the nanoparticles are not perfect, but displacement of atomic position from the proper site in the unit cell is taking place. We do not have a correct model for the atomic arrangements in the nanoparticle crystal currently. This is one of the important tasks for analyzing multi-scale functional materials from atomic scale to higher-order structures. After introducing a proper atomic structural model of the deformation, we will be able to fit whole scattering/diffraction pattern from SAXS to WAXS as shown in Fig. 4 (WAXS fitting needs a better model as well).

2.2. SAXS analysis for PEM structure

Conductivity of protons in PEM is one of the important parameters that restrict kinetics in the fuel cell. It is thought that protons are transferred through network of water channels in PEM, which is formed in the high-humidity conditions in the fuel cell. In order to study the real mechanism of proton transport, we need to investigate nanometer-scale structural changes of the PEM at the operating condition of the cell, that is, typically at 80°C and high humidity. SAXS is well suited for investigating nanometer-scale structures such as formation of proton transport channel, using an X-ray transmission *in situ* sample cell. Mochizuki *et al.* reported an *in situ* SAXS study[10] investigating structural change of four PEM films with increasing humidity from 20% to 90% at 80°C. Those four films are classified into two-types: perfluorosulfonic acid polymer (Nafion and Aquivion) and sulfonated aromatic acid polymer (SPE-*bl*-1 and SPK-*bl*-1). The observed SAXS profiles for those PEM films are shown in Fig. 5. With rising humidity, water uptake of those films increases and the nanometer-scale structure of the films should be affected. In the case of perfluorosulfonic acid polymers, which are shown in Fig. 5(a) Nafion and (b) Aquivion, the first low angle peak corresponds to the distance between the crystalline domains and the second, higher angle peak is considered to be the correlation between ionic domains (the so called ionomer peak). The intensity of the high angle peak increases and it moves to lower angle with rising humidity. This means the ionic domain is expanding with increasing water uptake in PEM. The growth of the ionic domain could make a more solid proton-transport channel and enhancing the conductivity of protons. Such behavior is consistent with increasing proton conductivity with rising humidity[10]. In the case of sulfonated aromatic acid polymers shown in Fig. 5(c) SPE-*bl*-1 and (d) SPK-*bl*-1, the SAXS pattern behavior is more complex. At first, we notice the peak position is much lower than that of perfluorosulfonic acid. It means distance between ionic

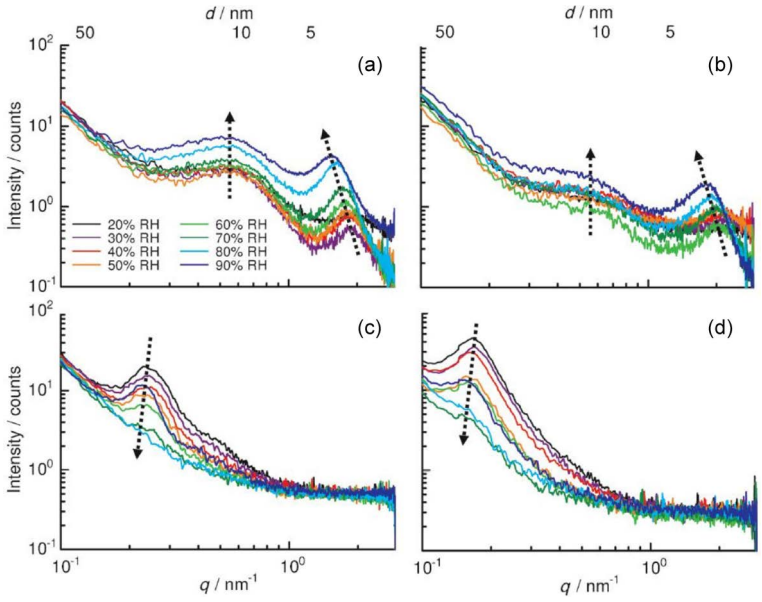

Fig. 5. Small angle scattering profiles for different kind of polymer membranes with changing humidity at 80°C[10].

domains are much larger (25.7 nm for SPE-*bl*-1 and 38.2 nm for SPK-*bl*-1) than that of Nafion (4.0 nm) and Aquivion (3.5 nm). Those differences are also confirmed with transmission electron microscope images[10]. Within the range of humidity from 20% to 80%, the ionomer peaks are weakened with rising humidity. This indicates the ionic domain becomes random with increasing water uptake in this humidity range. However, the peak intensity becomes greater at 90% or more humidity. This is consistent with the observation that proton conductivity of sulfonated aromatic acids becomes higher at the highest humidity condition. We can investigate structural change of various PEMs with SAXS and find to know proper operating condition for those PEMs.

SAXS is also useful to study the structure of the catalyst support, which has characteristic dimension of several tens of nanometers in order to increase surface area within limited volume. The support has two important functions. One is effective supply of the H_2 and O_2 gases to the catalyst particles, and the other is good electrical conductivity to pickup and supply electrons. Currently graphite is used for the support material. However, it is a problem for the cathode support because it can easily react with H_2O molecules and create CO_2 while the fuel cell is operating at high-voltage. This situation occurs when the fuel cell is started or stopped, and results in graphite evaporation. For prolonging the lifetime of fuel cells, much more robust support materials are needed. Therefore, a number of metal oxides have been studied to find a superior material[11]. Senoo *et al*. proposed that Nb-doped SnOx ($x=2-\delta$) is a promising candidate for the support[12]. They pointed out that the network structure is key for obtaining large surface area and high electrical conductivity. SAXS and USAXS are suited to investigate such multi-scale structures from few nanometers to several hundreds nanometers. However, it is difficult to obtain key physical parameters such as surface area, connectivity, *etc*. and there is a need to develop analysis methods for such multi-scale complex structures from scattering (SAXS, USAXS) data.

3. Observation by X-ray microscopy

3.1. Investigation for MEA structure

In the previous section, we reviewed the observations from scattering and diffraction from atomic-scale to several tens of nanometer-scale structures. In this section, we will introduce observations for micrometer-scale structures in the fuel cell. Figure 6 shows a cross-sectional view of the MEA obtained by X-ray computed tomography (CT) using the Rigaku nano3DX. The stacking structure shown schematically in Fig. 1, PEM is sandwiched by anode and cathode catalyst layers (CLs) and GDL layers, is clearly recognized. In this CT image, the area indicated by a brighter color has a higher X-ray absorption coefficient and the dark area is the opposite. In this specimen, an additional micro-porous layer (MPL) is inserted between the catalyst and GDL layers. The MPL has a number of pores a few nanometers in diameter. This layer has the function of efficiently diffusing water from the CL to the GDL, and allow for operating in the higher-current regime without dropping the output voltage.

The three-dimensional view of the same MEA is shown in Fig. 7. We can easily recognize the whole MEA structure with this image and notice bright areas in the cathode CL. This should be condensation of catalyst metal nanoparticles. Figure 8 also shows different cross-sectional views, perpendicular to that shown in Fig. 6. As seen in Fig. 8(a), carbon fibers, several micrometers in diameter, are dispersed thinly and maintaining gas and water-flow channels. From Fig. 8(b) to 8(c), the transition from the region where the GDL and MPL coexist to MPL only is shown, and cracks in the MPL are seen. Brighter areas are noticed in the CL shown in Fig. 8(d). This is because heavy metal particles are present. Condensation of catalyst is also noticeable. As shown in this section, the MEA is complex structure and each constituent component has a key role in a well performing fuel cell. X-ray CT, with reasonably high-resolution, is able to visualize those key components and is quite useful to investigate an actual working fuel cell.

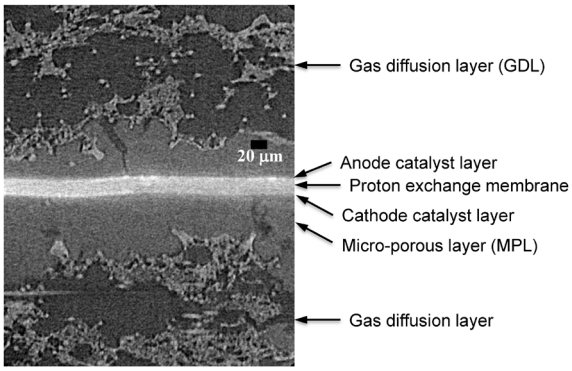

Fig. 6. Cross-section CT image for membrane electrode assembly (MEA). The structure shown in Fig. 1 is clearly recognized.

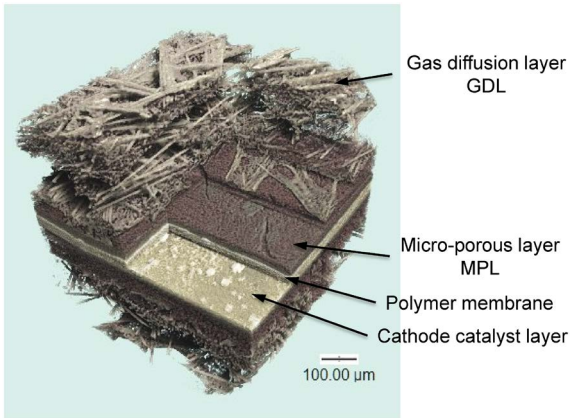

Fig. 7. Three-dimensional visualization of the MEA structure obtained by CT measurement.

3.2. *In operando* observation of working fuel cell

In a working fuel cell, the flow of generated water seriously affects continuous operation and constant generation of electricity. The water should be removed smoothly without any effect on H_2 flow during operation. Professor Hirai and his group are intensively studying visualization of liquid water flow in the working fuel cell with *in operando* X-ray microscopy observation[13]. For example, they investigated the effect of the MPL from the perspective of water flow and found it has a function to prevent water condensation at the CL interface even at the condition of higher current operation. The MPL is also working for maintaining smooth water flow to GDL[14]. These observations provide valuable information for the actual reactions in the fuel cell. However, their observations use a microfocus X-ray source and obtain high special resolution image with geometrical expansion as shown in Fig. 9(b). The difference of magnification between near-side and far-side from the source is noticeable and it is not possible to define where is the interface in Fig. 9(a). On the other hand, the nano3DX uses a parallel beam geometry[4] and there are no differences in the image for near-side and far-side from the source as shown in Fig. 9(c). The nano3DX is thus able to define where liquid water is located. Currently, Rigaku is collaborating with Professor Hirai's group for visualizing the liquid water and determine the

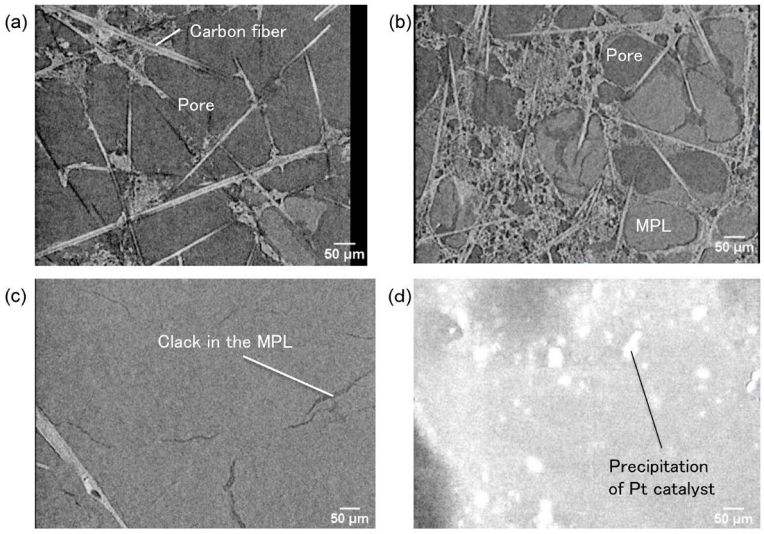

Fig. 8. Tomography images of (a) GDL, (b) GDL/MPL zone, (c) MPL, (d) catalyst layer.

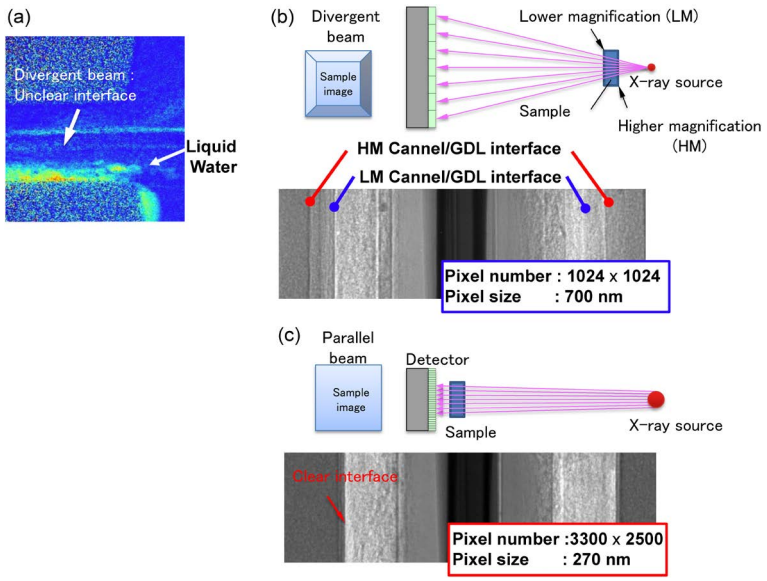

Fig. 9. Visualization of water flow in the fuel cell while generating electric power. (a) Water flow obtained by divergent X-ray beam projection. (b) Schematic and real image of divergent beam projection. Interfaces of each layer are not clear due to the different magnifications at the near and far side. (c) Schematic and real image of parallel beam projection and interface areas are clearly identified and investigated.

exact position where it is created at the real operating conditions of a fuel cell to within a micrometer. This study is supported by NEDO†. We expect the Rigaku parallel beam X-ray microscope to provide a set of very useful observations in an operating fuel cell to improve lifetime and electric power generating performance of future fuel cells.

4. Conclusion

In this paper, we have presented observations of complex fuel cell structure over the range of atomic-scale to macroscopic-scale by utilizing X-ray scattering/diffraction and X-ray microscopy. These X-ray techniques can provide unique structural information without destroying the specimen and apply these techniques to *in operando* observation of a fuel cell. The spatial resolution of the recently improved X-ray microscope, nano3DX, is one micrometer or less and it is possible to observe multi-stacked complex MEA structure. Furthermore, we can trace creation and flow of liquid water in an operating fuel cell with high spatial resolution and this may contribute to improving fuel cell performance.

Acknowledgments

The authors would like to thank Professor S. Hirai, Research Center for Carbon Recycling and Energy, Tokyo Institute of Technology and Professor K. Kakinuma, Fuel Cell Nanomaterials Center, University of Yamanashi to provide valuable samples. We can learn a lot of things regarding structure and operation of fuel cell with their kind supports.

References

(1) K. Palczewski, T. Kumasawa, T. Hori, C. A. Behnke, H. Motoshima, B. A. Fox, I. L. Trong, D. C. Teller, T. Okada, R. E. Stenkamp, M. Yamamoto and M. Miyano: *Science*, **289** (2000), 739−745.
(2) M. Sakata and M. Sato: *Acta Cryst.*, **A46** (1990), 263−270.
(3) M. Gradzielski and A. J. Allen: *J. Apply. Cryst.*, **49** (2016), 1858−1860, and references therein.
(4) Y. Takeda and K. Hamada: *Rigaku Journal (English version)*, **30** (2014), No. 1, 17−22.
(5) K. Omote, Y. Takeda, R. Hirose and J. Ferrara: *Rigaku Journal*, **33** (2017), No. 1, 4−9.
(6) Y. Wang, K. S. Chen, J. Mishler, S. C. Cho and X. C. Adroher: *Applied Energy*, **88** (2011), 981−1007.
(7) H. F. M. Mohamed, Y. Kobayashi, C. S. Kuroda and A. Ohira: *J. Membrane Sci.*, **360** (2010), 84−89.
(8) T. Toda, H. Igarashi, H. Uchida and M. Watanabe: *J. of The Electrochemical Society*, **146** (1999), 3750−3756.
(9) N. Ishiguro, T. Saida, T. Uruga, S. Nagamatsu, O. Sekizawa, K. Nitta, T. Yamamoto, S. Ohkoshi, Y. Iwasawa, T. Yokoyama and M. Tada: *ACS Catalysis*, **2** (2012), 1319−1330.
(10) T. Mochizuki, K. Kakinuma, M. Uchida, S. Deki, M. Watanabe and K. Miyatake: *ChemSusChem*, **7** (2014), 729−733.
(11) Y. Liu and E. Mustain: *J. Am. Chem. Soc.*, **135** (2013), 530−533.
(12) Y. Senoo, K. Kakinuma, M. Uchida, H. Uchida, S. Deki and M. Watanabe: *RSC Advances*, **4** (2014), 32180−32188.
(13) T. Sasabe, S. Tsushima and S. Hirai: *Int. J. Hydrogen Energy*, **35** (2010), 11119−11128.
(14) P. Deevanhxay, T. Sasabe, S. Tsushima and S. Hirai: *J. Power Source*, **230** (2013), 38−43.

† New Energy and Industrial Technology Development Organization in Japan